Efficient Wideband MRCS Simulation for Radar HRRP Target Recognition Based on MSIB and PCA

Yunqin Hu * and Ting Wan

Department of Communication Engineering
Nanjing University of Posts and Telecommunications, Nanjing, 210009, China
*huyq@njupt.edu.cn

Abstract ─ In this paper, efficient wideband monostatic radar cross-section (MRCS) simulation is presented for radar high range resolution profile (HRRP) target recognition. Firstly, an efficient numerical approach is proposed for the wideband MRCS. The well-conditioned integral equation and the higher-order hierarchical divergence-conforming vector basis functions are utilized for the scattering field. The adaptive cross approximation (ACA) based matrix compression method is applied for efficient analysis of MRCS at a specific frequency point. The geometric theory of diffraction (GTD) based scattering model is utilized for MRCS over a wide frequency band. Secondly, the radar HRRP target identification is performed by using principal component analysis (PCA) on modified surrounding-line integral bispectrum (MSIB). The HRRP of target can be obtained by inverse fast Fourier transform (IFFT) of the spectral domain backscattering field within a certain frequency range. The one-dimensional MSIB features of HRRP are extracted to constitute eigenvectors for radar target recognition. To enhance the separation ability of radar target recognition, the MSIB is projected onto PCA space before recognition. Numerical examples prove that the proposed algorithm is feasible and efficient.

Index Terms ─ Adaptive cross approximation, geometric theory of diffraction, high range resolution profile, modified surrounding-line integral bispectrum, principal component analysis.

I. INTRODUCTION

The high range resolution profile (HRRP) carries information of target scattering centers distribution along the radar line-of-sight, reflecting details of target structure such as scatter centers' strength, scatter centers' position, target size, and so on. These target features have been shown to be highly discriminative. HRRP based radar target recognition has received extensive attention and research [1-3].

In the field of non-cooperative radar HRRP target recognition, various computational electromagnetics algorithms have been widely used in the prediction of scattered electromagnetic fields of actual targets. Frequency domain surface integral equation (SIE) by the method of moments (MoM) is a powerful tool in full wave electromagnetic simulation, since it does not need to handle the absorbing boundary conditions and its computational domain is taken on the surface of the target. Most of the existing fast methods for surface integral equations, such as the multilevel fast multipole algorithm (MLFMA) [4], are based on the fact that when unknowns N are grouped in local spatial regions, the resulting blocks of the system impedance matrix $\mathbf{Z}$ are rank deficient. It is noteworthy that in radar HRRP target recognition, the wideband monostatic radar cross-section (MRCS) must be simulated. Since the scattering field depends on both frequency and incident angle, most of the available iterative algorithms must be run at each incident angle and frequency point many times. Obviously, the repeated solution of linear systems is time-consuming and expensive.

Many efforts have been done to accelerate the wideband MRCS simulation. For monostatic scattering at a specific sample frequency point, two classes of methods are mainly studied. One is the interpolation method, including the asymptotic waveform evaluation (AWE) technique [5,6] and the cubic-spline method [7]. The other is the matrix compression method. When unknowns are spatially grouped, the rank deficient interaction submatrices between well-separated groups can be well approximated as the outer product of two lower rank matrices. For monostatic scattering, where there are many right-hand sides (RHS), the blocked RHS can be also well approximated by this low rank outer product form where each outer product approximant is computed using the adaptive cross approximation (ACA) [8]. For wideband scattering analysis, impedance matrix interpolation [9], asymptotic waveform evaluation (AWE) technique [10] and Taylor expansion based method [11] are studied to reduce the total simulation time.

The HRRP of target can be obtained by inverse fast Fourier transform (IFFT) to the simulated wideband MRCS. However, due to the shift sensitivity, the

Submitted On: May 9, 2018
Accepted On: November 28, 2019

translation invariance features reflecting the essential features of HRRP must be extracted from the original data before recognition. Fortunately, the bispectrum of HRRP has translation invariance while maintaining phase information and suppressing the additive white Gaussian noise (AWGN). However, using the bispectrum features for target recognition is inefficient, because it is a two-dimensional function and its data amount is the square of HRRP's. Many integral bispectrum methods have been developed to convert a bispectrum from two-dimensional to one-dimensional, including radially integrated bispectra (RIB) [12], axially integrated bispectra (AIB) [13], circularly integrated bispectra (CIB) [14] and surrounding-line integral bispectrum (SIB) [15]. Compared with the others, SIB is more preferred because its integration path contains all the information of bispectrum, with no missing or reusing any bispectrum information, and avoids any interpolation in the integration process. By choosing integral paths exactly consistent with the bispectrum symmetry, the modified surrounding-line integral bispectrum (MSIB) has less computational complexity than SIB [16].

This paper is organized as follows. In Section II, an efficient numerical approach is proposed for wideband MRCS. Firstly, the well-conditioned integral equation and the novel higher-order hierarchical divergence-conforming vector basis functions are utilized for efficient analysis of electromagnetic scattering. Then, the matrix compression method based on ACA and the scattering model based on the geometric theory of diffraction (GTD) are employed to improve the simulation efficiency of wideband MRCS. In Section III, the MSIB features of HRRP are extracted to constitute eigenvectors for target identification. To enhance the separation ability of radar target recognition, the MSIB features are projected onto the PCA space before recognition. Numerical simulations are used to demonstrate the feasibility and effectiveness of the approach in Section IV. Finally, the conclusion is given in Section V.

II. ANALYSIS OF WIDEBAND MRCS

A. Integral equation and basis function

The combined field integral equation (CFIE) has been used extensively for conducting bodies. For a homogenous dielectric object, the Poggio-Miller-Chang-Harrington-Wu-Tsai (PMCHWT) [17] formulation is widely used, because it can yield an accurate solution without the interior resonance corruption. However, PMCHWT suffers from poor convergence problems [18]. In this paper, the electric-magnetic current combined-field integral equation (JMCFIE) which provides better conditioned system matrix for iterative solution is utilized to analyze electromagnetic scattering from a homogeneous dielectric target.

Using the equivalence principle, the homogeneous dielectric scattering problem can be solved by considering two simple equivalent problems, an external equivalent problem in the free space denoted by D_1 and an internal equivalent problem in the unbounded homogeneous dielectric domain D_2 characterized by $(\varepsilon_r, \mu_r, \sigma_r)$. Let $\mathbf{n}_l$ denote the unit normal of the object surface pointing into domain D_l. A set of integral equations can be formulated for each equivalent problem. For the exterior equivalent problem, they are the electric field integral equation (EFIE) and the magnetic field integral equation (MFIE), denoted as EFIE_1 and MFIE_1. For the internal equivalent problem, the integral equations for electric and magnetic field are denoted as EFIE_2 and MFIE_2 [19, 20]. In PMCHWT formulation, the EFIE_1 is combined with the EFIE_2 to form a combined equation. Similarly, the MFIE_1 is combined with the MFIE_2 to form another combined equation.

The well-conditioned JMCFIE formulation can be established by combining the interior and exterior equivalent problems as the following form [21]:

$$\begin{cases} \dfrac{1}{\eta_1}\mathrm{EFIE}_1 + \mathbf{n}_1 \times \mathrm{MFIE}_1 + \dfrac{1}{\eta_2}\mathrm{EFIE}_2 + \mathbf{n}_2 \times \mathrm{MFIE}_2 \\ -\mathbf{n}_1 \times \mathrm{EFIE}_1 + \eta_1 \mathrm{MFIE}_1 - \mathbf{n}_2 \times \mathrm{EFIE}_2 + \eta_2 \mathrm{MFIE}_2 \end{cases}, \quad (1)$$

where $\eta_l = \sqrt{\mu_l / \varepsilon_l}\,(l = 1, 2)$.

In terms of the geometrical modeling and current discretization, traditional methods are low-order techniques using plane triangle patches and low-order basis functions, such as the Rao-Wilton-Glisson basis function (RWG). For electrically large size problems, the accuracy of solutions obtained by low-order techniques can only be improved slowly with the increase of unknowns, thus, the number of unknowns will be very large inevitably. To resolve such problems, the higher-order hierarchical divergence-conforming vector basis functions defined on curved triangular patches are used in this paper.

First, choose the curve Rao-Wilton-Glisson basis function (CRWG) as the lowest-order (order-0.5) divergence-conforming basis function. It can be expressed in normalized area coordinates (ξ_1, ξ_2, ξ_3) as:

$$\begin{aligned} \mathbf{f}^e_{1,0}(\mathbf{r}) &= \frac{1}{J}\left[(\xi_1 - 1)\frac{\partial \mathbf{r}}{\partial \xi_1} + \xi_2 \frac{\partial \mathbf{r}}{\partial \xi_2}\right] \\ \mathbf{f}^e_{2,0}(\mathbf{r}) &= \frac{1}{J}\left[\xi_1 \frac{\partial \mathbf{r}}{\partial \xi_1} + (\xi_2 - 1)\frac{\partial \mathbf{r}}{\partial \xi_2}\right] \\ \mathbf{f}^e_{3,0}(\mathbf{r}) &= \frac{1}{J}\left[\xi_1 \frac{\partial \mathbf{r}}{\partial \xi_1} + \xi_2 \frac{\partial \mathbf{r}}{\partial \xi_2}\right], \end{aligned} \quad (2)$$

where J is the element Jacobian and $\mathbf{r}$ is the position vector of the point determined by normalized face coordinates on curved parametric triangular patch.

The novel higher-order bases are constructed by multiplying the corresponding order new orthogonal scalar polynomials with the lowest order bases [22, 23]. The order of basis function is 0.5 higher than that of polynomials. Without loss of generality, we consider basis functions associated with edge 1. The edge-based basis functions of order-3.5 associated with edge 1 can be expressed as:

$$\begin{aligned}
\mathbf{f}^e_{1,1}(\mathbf{r}) &= \sqrt{3}(\xi_2-\xi_3)\mathbf{f}^e_{1,0}(\mathbf{r}) \\
\mathbf{f}^e_{1,2}(\mathbf{r}) &= \frac{\sqrt{5}}{2}\left[3(\xi_2-\xi_3)^2-1\right]\mathbf{f}^e_{1,0}(\mathbf{r}) \\
\mathbf{f}^e_{1,3}(\mathbf{r}) &= \frac{\sqrt{7}}{2}\left[5(\xi_2-\xi_3)^3-3(\xi_2-\xi_3)\right]\mathbf{f}^e_{1,0}(\mathbf{r}).
\end{aligned} \tag{3}$$

As in Formula (2), the superscript of $\mathbf{f}^e_{i,j}$ denotes edge-based, the subscript *i* denotes the number of the edge and *j* denotes the order of hierarchical polynomials.

The face-based basis functions of order-3.5 associated with edge 1 can be expressed as:

$$\begin{aligned}
\mathbf{f}^f_{1,01}(\mathbf{r}) &= 2\sqrt{3}\xi_1\mathbf{f}^e_{1,0}(\mathbf{r}) \\
\mathbf{f}^f_{1,02}(\mathbf{r}) &= 2\sqrt{3}\xi_1(5\xi_1-3)\mathbf{f}^e_{1,0}(\mathbf{r}) \\
\mathbf{f}^f_{1,11}(\mathbf{r}) &= 6\sqrt{5}\xi_1(\xi_2-\xi_3)\xi_1\mathbf{f}^e_{1,0}(\mathbf{r}) \\
\mathbf{f}^f_{1,03}(\mathbf{r}) &= 2\sqrt{30}\xi_1(2-8\xi_1+7\xi_1^2)\mathbf{f}^e_{1,0}(\mathbf{r}) \\
\mathbf{f}^f_{1,12}(\mathbf{r}) &= 2\sqrt{30}(\xi_2-\xi_3)\xi_1(7\xi_1-3)\mathbf{f}^e_{1,0}(\mathbf{r}) \\
\mathbf{f}^f_{1,21}(\mathbf{r}) &= 2\sqrt{210}(\xi_2^2-4\xi_2\xi_3+\xi_3^2)\xi_1\mathbf{f}^e_{1,0}(\mathbf{r}).
\end{aligned} \tag{4}$$

The superscript of $\mathbf{f}^f_{i,mn}$ denotes face-based, the first subscript *i* denotes the number of the edge, and the sum of two digits of the second subscript is equal to the order of the polynomial.

The edge-based and face-based basis functions associated with edge 2 and edge 3 can be obtained by rotating the coordinates, $\xi_1 \to \xi_2 \to \xi_3 \to \xi_1$ in (3) and (4), and then multiplying the corresponding lowest-order basis in (2). Note that one of the three subsets of face-based functions should be discarded since a 2-D triangle element can have only two independent tangent vectors. The hierarchical divergence-conforming vector basis functions of order-3.5 include the vector basis functions of order-2.5 and order-1.5.

After expanding the equivalent surface current densities with the higher-order hierarchical divergence-conforming vector basis functions and using the Galerkin's testing procedure, the integral equation can be well tested leading to a matrix equation:

$$\mathbf{A}\cdot\mathbf{x}=\mathbf{b}, \tag{5}$$

where **A** is the impedance matrix, **x** is the unknown coefficient vector of the basis function, **b** is the excitation vector generated by the incident wave.

Comparing with the low-order techniques, the novel higher order hierarchical divergence-conforming vector basis function can greatly reduce the number of unknowns for a given problem. To reduce the memory requirement and computational complexity of MoM, the MLFMA is employed to complete the matrix-vector product of each iteration step. The FMM box size must be chosen to be a little bit larger than the average patch size [24].

B. ACA for MRCS

Iterative solvers may be quite satisfactory for only a few RHS such as bistatic problems, but for monostatic scattering with many required sampling angles, this part of the problem becomes expensive, because iterative solvers must be used to compute current solutions for each RHS excitation vector.

For analyzing the MRCS at a given operating frequency, the impedance matrix remains the same, whereas the RHS vector should be updated at each incident angle. The MRCS problem can be expressed in the following matrix form:

$$\mathbf{A}\cdot\mathbf{X}=\mathbf{B}, \tag{6}$$

where $\mathbf{B}=[\mathbf{b}_1, \mathbf{b}_2,\ldots,\mathbf{b}_M,]$, $\mathbf{X}=[\mathbf{x}_1, \mathbf{x}_2,\ldots, \mathbf{x}_M,]$ and *M* is the number of incident angles.

Like the impedance matrix, the blocked RHS is also low rank and can be compressed by the ACA method. Readers can see [8] for Bebendorf's ACA details. By using ACA, the blocked RHS can be approximated using low rank representations:

$$\mathbf{B}\approx\mathbf{U}_{\mathrm{ACA}}\cdot\mathbf{V}_{\mathrm{ACA}}. \tag{7}$$

The dimension of matrices $\mathbf{U}_{\mathrm{ACA}}$ and $\mathbf{V}_{\mathrm{ACA}}$ are $N\times k$ and $M\times k$, respectively. Generally, *k* is much smaller than *M*. By substituting (7) into (6), the linear equations can be rewritten as:

$$\mathbf{X}\approx\left(\mathbf{A}^{-1}\cdot\mathbf{U}_{\mathrm{ACA}}\right)\cdot\mathbf{V}^{\mathrm{H}}_{\mathrm{ACA}}. \tag{8}$$

The iterative solution of linear equations $\mathbf{A}^{-1}\cdot\mathbf{U}_{\mathrm{ACA}}$ is required at each principle eigenvectors. Compared with solving linear equations at each angle repeatedly, the ACA method is able to greatly reduce the computation time. The computational complexity of ACA is $k^2(N+M)$ and the memory requirement is $k(N+M)$.

C. GTD-based scattering model for wideband MRCS

In radar HRRP target recognition, MRCS must be simulated at multiple frequency sampling points over wideband. Since the impedance matrix depends on frequency, the above electromagnetic algorithm must be repeated at each frequency point. To improve simulation efficiency, a parametric scattering model based on the GTD is utilized for fast analysis of the scattered field over a wide frequency band.

In GTD method [25], the backscattering from a target, which can be modeled as a collection of ideal scattering centers, can be approximated as:

$$E^{sca}(f)=\sum_{m=1}^{M}b_m\left(j\frac{f}{f_c}\right)^{\alpha_m}e^{\left(-j\frac{4\pi}{c}fr_m\right)}, \quad (9)$$

where, M denotes the order of the model; b_m and r_m denotes the complex scattering amplitude and vertical distance of the mth scattering center; f_c is the center frequency of the test band; α_m is an integer multiple of 0.5, which reflects the scattering mechanism of the scattering center.

For real targets, when data are collected over a very narrow angular window, (9) still provides a very compact way to model their backscattering. However, when data collected over a broad angular window, if we want to model a complex target as a summation of ideal scattering centers, we have to use a different set of scattering centers for each different observation angle. The backscattering can be approximated as the summation of point scatterers multiplied by their respective aspect-dependent amplitude functions [26]:

$$E^{sca}(f,\theta,\varphi)=\sum_{m=1}^{M}b_m(\theta,\varphi)\left(j\frac{f}{f_c}\right)^{\alpha_m}e^{\left(-j\frac{4\pi}{c}fr_m\right)}. \quad (10)$$

The amplitude function $b_m(\theta,\varphi)$ for each scattering center accounts for angular dependence and must be stored. The parameters of GTD scattering center model can be extracted from the scattered field at partial sampling frequency points by using the matrix pencil method [27].

III. TARGET RECOGNITION BASED ON MSIB AND PCA

Suppose that the spectral backscatter field of N_F sampling frequency points at a specific sampling angle can be expressed as $\mathbf{X}=[X(1), X(2), \ldots, X(N_F)]^T$. The HRRP can be obtained by IFFT:

$$\mathbf{x}=\left[|x(1)|,|x(2)|,...,|x(N_F)|\right]^T, \quad (11)$$

$$\mathbf{x}(n)=IFFT\left[\mathbf{X}(n)\right], \quad n=1,2,...,N_F. \quad (12)$$

The bispectrum of HRRP is defined as the Fourier transform of the third-order cumulant of HRRP sequence:

$$B(\omega_1,\omega_2)=X(\omega_1)X(\omega_2)X^*(\omega_1+\omega_2), \quad (13)$$

$$X(\omega)=\sum_{\tau=-\infty}^{\infty}x(\tau)\exp(-j\omega\tau). \quad (14)$$

The bispectrum is translation invariant, while maintaining the phase information and inhibiting the AWGN theoretically. However, bispectrum is a two-dimensional function and its data amount is the square of HRRP's. If the two-dimensional bispectrum features is directly used in target recognition, a large amount of memory is needed for the target template library. In addition, the bispectrum has great information redundancy.

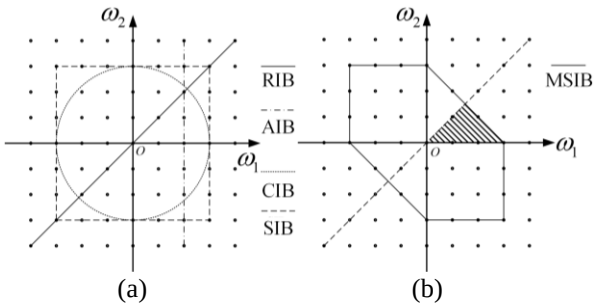

Fig. 1. Integral path of the different integrated bispectra: (a) RIB, AIB, CIB, SIB, and (b) MSIB.

To decrease the computational complexity of target recognition, many different integral bispectrum methods have been developed to convert a bispectrum from two-dimensional to one-dimensional. According to the integral path, four kinds of integral bispectrum are shown in Fig. 1 (a), with each point represents a value of bispectrum. The calculation of the integral bispectrum can be simplified by using the bispectrum symmetry.

According to the periodicity and symmetry of bispectrum, bispectrum in $0\le\omega_1\le\omega_2\le\omega_1+\omega_2\le\pi$ contains all the information. As shown in Fig. 1 (b), the MSIB integrates along a closed hexagons centered at the origin. The MSIB does not omit or reuse any bispectrum values, so as to ensure that important information can be obtained for target recognition. The MSIB expression is:

$$\mathrm{MSIB}(s)=\sum_{R_s}B(\omega_1,\omega_2), \quad s=1,2,...,m, \quad (15)$$

where R_S is an integral path and m is the total number of integral paths. Because the path of integration completely conforms to the bispectrum symmetry, it only needs to integrate along the section within the shaded area. This makes the time of extracting integral bispectrum features significantly saved.

Suppose the total number of targets is C. By simulating the backscattering responses of each target at n_c sampling angles, n_c training samples of MSIB will be obtained for target c, c=1, 2, …, C. The training samples of these targets form a MSIB database $\mathbf{X}=\{\mathbf{x}_1, \ldots, \mathbf{x}_i, \ldots, \mathbf{x}_N\}$, where $\mathbf{x}_i$ represents a MSIB vector of some target. The total number of training samples is $N=\sum_{c=1}^{C}n_c$. The MSIB can be used as feature vectors of targets, but bispectrums on many integration paths may be redundant, and some are even baneful for target classification.

The PCA is utilized to reduce the redundant information and the feature space dimension of MSIB before recognition [28]. PCA seeks the most expressive features for well representing different classes with minimum mean square error. The mean vector and the

covariant matrix of the training samples are defined as:

$$\boldsymbol{\mu} = \frac{1}{N}\sum_{n=1}^{N}\mathbf{x}_n, \tag{16}$$

$$\mathbf{C} = \frac{1}{N}\sum_{n=1}^{N}(\mathbf{x}_n - \boldsymbol{\mu})\cdot(\mathbf{x}_n - \boldsymbol{\mu})^T, \tag{17}$$

where 'T' denotes the transpose. Then, compute the eigenvalue equation of the covariance matrix:

$$\mathbf{C}\mathbf{p} = \lambda\mathbf{p}. \tag{18}$$

Assume that the eigenvalues are arranged from maximum to minimum, $\lambda_1 \geq \lambda_2 \geq ... \geq \lambda_m \geq 0$, and the corresponding eigenvectors are $\mathbf{p}_1$, $\mathbf{p}_2$, …, $\mathbf{p}_m$. The transformed matrix is constituted with the eigenvectors corresponding to the previous n_{PCA} eigenvalues:

$$\mathrm{A} = \left(\mathbf{p}_1, \mathbf{p}_2, ..., \mathbf{p}_{n_{PCA}}\right)^T, \quad n_{PCA} < m. \tag{19}$$

Each MSIB vector can be projected onto the n_{PCA}-dimensional PCA space by the following formula:

$$\mathbf{y}_i = \mathbf{A}(\mathbf{x}_i - \boldsymbol{\mu}). \tag{20}$$

In this way, the dimension of the MSIB vectors is decreased to n_{PCA}. Then, the radar recognition is performed by the maximal correlate coefficient template marching method (MCC-TMM) on the low-dimensional PCA space. The recognition accuracy depends on n_{PCA}. Generally, the larger the n_{PCA}, the higher the recognition accuracy, but there is no optimum selection rule to maximize the probability of correct recognition while retaining a small value [29]. This will be discussed in the next section.

IV. NUMERICAL SIMULATION

In this section, numerical examples are given to verify the valid and efficiency of the proposed method. In all examples, the inner-outer Flexible Generalized Minimal Residual (FGMRES) method is used for the iterative solution, where the inner and outer restart numbers are both taken to be 10, and the stop precision for the inner and outer iteration is 1.E-2 and 1.E-4, respectively.

Firstly, the accuracy and validity of the well-conditioned integral equation combined with the novel higher-order hierarchical divergence-conforming vector basis functions and the MLFMA are verified by a dielectrically coated warhead model ($\varepsilon_r = 2.0$), as shown in Fig. 2. The incident plane wave is 3GHz and the incident angels are θ_i=0°, φ_i=0°. For composite conducting and dielectric object, the CFIE on the conductor surface and the JMCFIE on the dielectric surface are combined, noted as JMCFIE-CFIE. The novel higher-order hierarchical divergence-conforming vector basis functions and the MLFMA are utilized for efficient analysis. Corresponding to order-1.5, order-2.5 and order-3.5 hierarchical bases, 46390, 38598 and 35712 unknowns are generated from curvilinear triangular patches discretization, respectively. The bistatic RCS for $\hat{\varphi}\hat{\varphi}$-polarization at φ_s=0° is computed and compared with low-order RWG method. As shown in Fig. 3, there is an excellent agreement between novel higher-order bases and RWG bases.

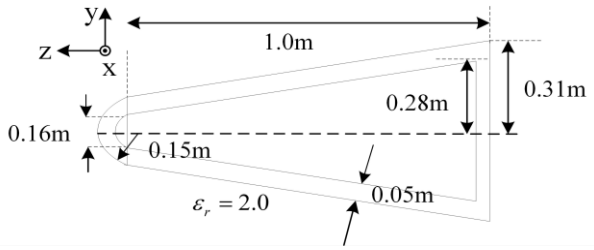

Fig. 2. Geometrical models for a dielectrically coated warhead.

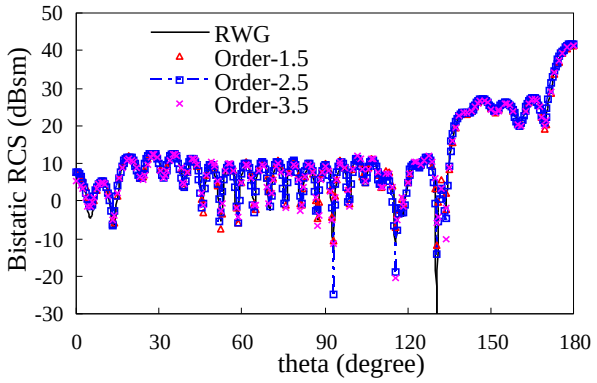

Fig. 3. Bistatic RCS for $\hat{\varphi}\hat{\varphi}$-polarization of a dielectrically coated warhead at 3 GHZ, with the RWG basis functions, order-1.5, order-2.5 and order-3.5 hierarchical basis functions.

Table 1: Memory requirements of MLFMA with different bases for dielectrically coated warhead

Bases	RWG	Order-1.5	Order-2.5	Order-3.5
Patch size (λ)	0.1	0.5	0.8	1.06
Total unknowns	222,168	46,390	38,598	35,712
MoM memory (MB)	376,576	16,418	11,366	9,730
Box size (λ)	0.25	0.8	1.0	1.3
Near field memory (MB)	1384.5	662.2	750.2	1041.6
Far field memory (MB)	1047.2	713.3	903.0	1228.9
MLFMA memory (MB)	2431.7	1347.9	1653.2	2270.5

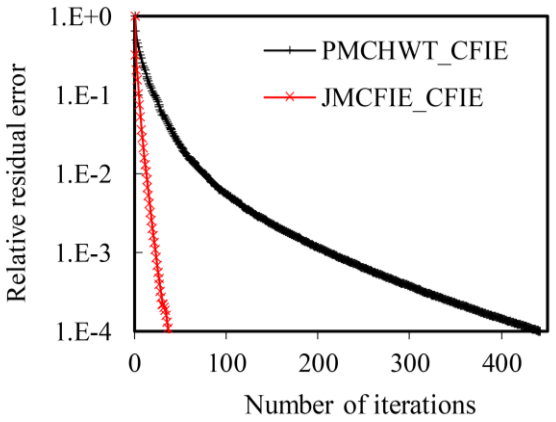

Fig. 4. Convergence histories of PMCHWT_CFIE and JMCFIE_CFIE solved with FGMRES for the dielectrically coated warhead.

The memory requirements of MLFMA are presented and compared between different bases in Table 1. With the increase of the order of higher-order basis functions, the total number of unknowns decreases, and the memory requirement of MoM greatly decreases, however, the near-field and far-field memory of MLFMA both increase. This is because, with the increase of the order of basis functions, the larger FMM box size is, and the larger the truncation term of MLFMA is, which leads to the low efficiency of MLFMA. After compromise consideration, order-1.5 and order-2.5 are more appropriate in the higher-order MLFMA. In the following numerical examples, the order of the hierarchical basis function is set to be 2.5. As shown in Fig. 4, the iterative convergence of JMCFIE-CFIE is plotted and compared with the traditional PMCHWT-CFIE. The latter needs 1829s and 444 iterative steps, while the former only needs 145s and 38 iterative steps. The result shows that the JMCFIE-CFIE has good iterative convergence characteristics.

Secondly, the accuracy and validity of the wideband MRCS algorithm are verified by a homogenous dielectric cylinder ($\varepsilon_r = 2.0, \mu_r = 1.0$) of 2.5m length and 0.6m diameter. The incident plane wave is 5GHz. As shown in Fig. 5, the MRCS for $\hat{\theta}\hat{\theta}$ -polarization is computed by the ACA based matrix compression method and compared with direct solution at each incident angle by FEKO. It can be found there is an excellent agreement. For direct solution, the iterative solver must be used at each incident angle and the total number is 361. While, for the ACA based matrix compression method, the iteration solver is only used 21 times, since the number of columns in $\mathbf{U}_{\mathrm{ACA}}$ is 21. This demonstrates that the ACA based matrix compression method can efficiently analyze the MRCS problem. In this example, the amount of calculation has been reduced by about 17 times. As shown in Fig. 6, the wideband backscattering for $\hat{\theta}\hat{\theta}$ -polarization of this dielectric cylinder is computed by the GTD-based scattering model and compared with and the direct solution at each sampling frequency point by FEKO. Good agreement can be found between them. The backscattering is computed at 81 equal spaced frequencies from 0.1GHz to 0.5GHz in FEKO, while the number of sampling frequencies is 21 in the GTD-based scattering model. In this example, the amount of calculation has been reduced by about 4 times, and plenty of time is saved by using the GTD-based scattering model.

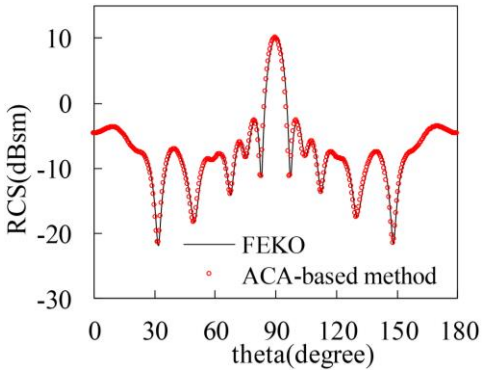

Fig. 5. MRCS for $\hat{\theta}\hat{\theta}$ -polarization of a dielectric cylinder ($\varepsilon_r = 2.0, \mu_r = 1.0$) of 2.5m length and 0.6m diameter at 5GHz.

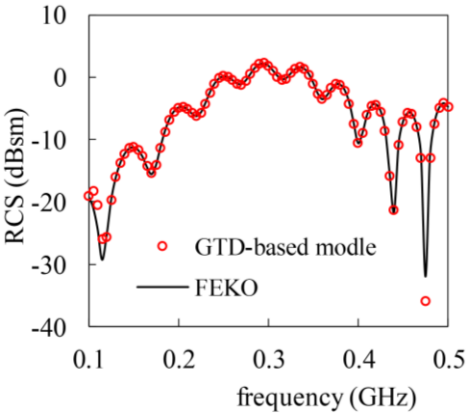

Fig. 6. Wideband MRCS for $\hat{\theta}\hat{\theta}$ -polarization of a dielectric cylinder ($\varepsilon_r = 2.0, \mu_r = 1.0$) of 2.5m length and 0.6m diameter at θ=0°.

Finally, numerical examples are given to verify the proposed radar recognition algorithm. Assume there are three known types of scaled aircraft models (i.e., *C*=3) including F15, F117 and VFY-218. The geometrical models and the geometry dimension for the three types of aircraft are shown in Fig. 7 and Table 2, respectively.

The $\hat{\theta}\hat{\theta}$ -polarization backscattering fields of these aircrafts are calculated by the proposed numerical approach in Section II. The elevation angle is fixed at 0°. The azimuth angle is changed continuously from 0° to 180° with an interval of 0.25°. At each azimuth angle, 161 frequency points from 1 to 5 GHz with a frequency step of 25 MHz are calculated. Thus, there are 721 HRRP corresponding to 721 azimuth angles for each target in the database, and the dimension of HRRP vector is 161.

With curvilinear triangular patches discretization, the unknown number of F15, F117 and VFY-218 for order-2.5 hierarchical basis functions is 187152, 153594 and 170898, respectively. The backscattering field of each aircraft at 21 frequency points uniformly distributed between 1G to 5G is calculated by the ACA based matrix compression method. Compared with solving linear equations repeatedly at 721 angles with direct solution, the iteration solver is only used 56, 41 and 48 times with the ACA accelerated method for F15, F117 and VFY-218, respectively. Plenty of iterative solution time can be saved. For wideband backscattering field, the GTD-based scattering model is established for each aircraft by using the backscattering field corresponding to 721 azimuth angles. Instead of computing at 161 frequency points with direct solution, the number of sampling frequency points is reduced to 21 by using the GTD-based scattering model. The computational efficiency has been improved by about 8 times. The HRRPs of each aircraft models are illustrated in Fig. 8. Figure 9 shows the bispectrums of F15 at φ=0° without and with AWGN (SNR=10dB), respectively. Figure 10 and Fig. 11 shows the bispectrums of F117 and VFY-218, respectively. It can be found from Fig. 9 to Fig. 11 that the estimation of bispectrum cannot completely suppress the AWGN. This is because when the length of pseudo-random sequence is limited, the third-order cumulant of Gaussian noise sequence approximately obeys the complex Gaussian distribution.

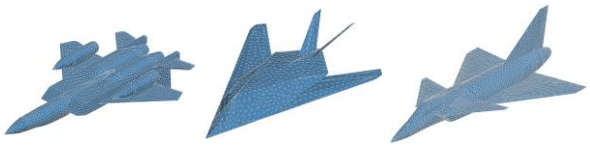

(a) (b) (c)

Fig. 7. Geometrical models for three known types of scaled aircraft: (a) F15, (b) F117, and (c) VFY-218.

Table 2: Dimension of scaled aircraft models (unit: m)

Aircraft	Length	Width	Height
F15	7.1713	5.0248	1.5967
F117	7.628	5.1547	0.9384
VFY-218	7.7354	4.4522	2.057

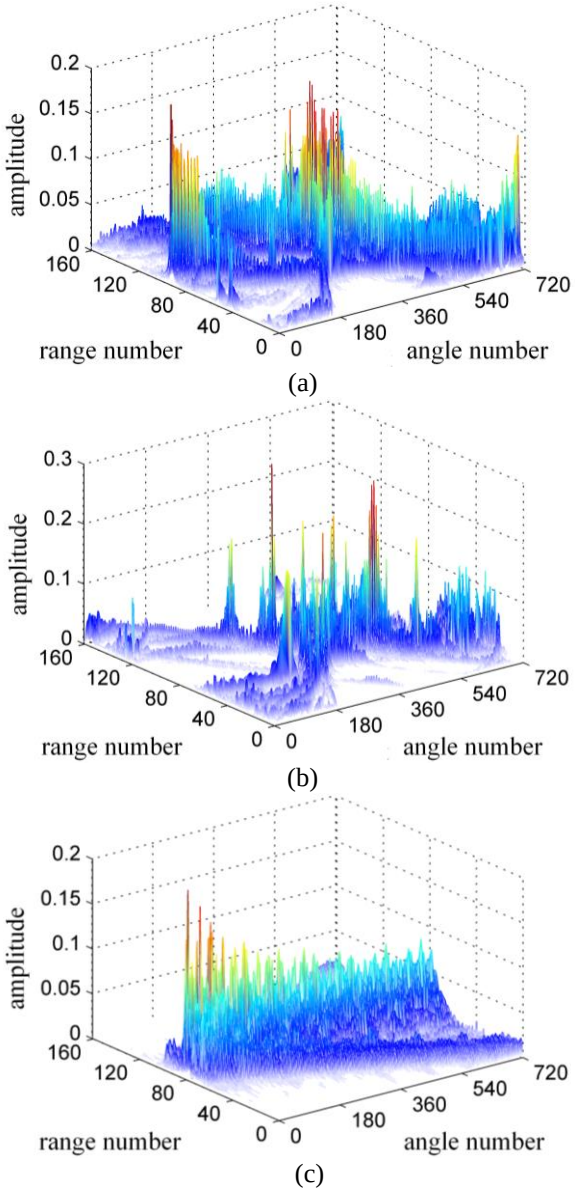

Fig. 8. HRRPs of the three aircraft models: (a) F15, (b) F117, and (c) VFY-218.

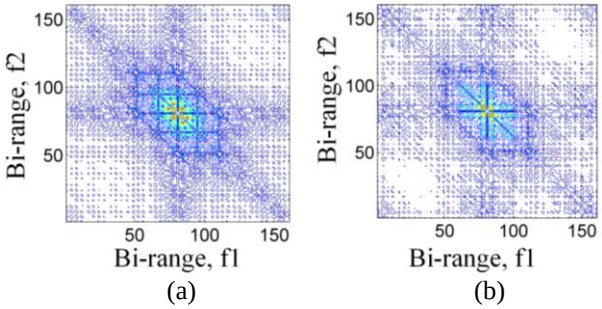

Fig. 9. Bispectrum for F15 at φ=0°: (a) without noise, and (b) with AWGN (SNR=10dB).

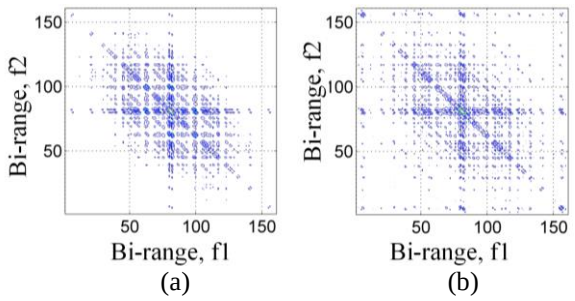

Fig. 10. Bispectrum for F117 at φ=0°: (a) without noise, and (b) with AWGN (SNR=10dB).

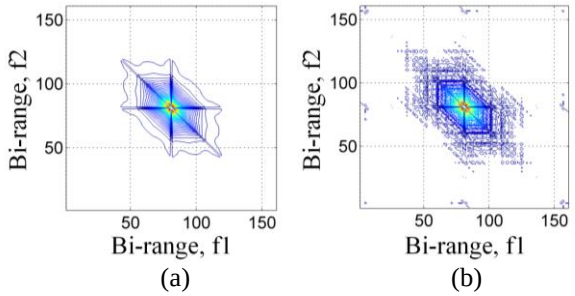

Fig. 11. Bispectrum for VFY-218 at φ=0°: (a) without noise, and (b) with AWGN (SNR=10dB).

We uniformly choose one in every three of the 721 MSIBs as the training samples, leading to 241 training samples for each target. The rest of the MSIBs in the database are served as testing samples, providing totally 1440 testing samples. Figure 12 shows the average correct recognition rates (CRR) of MSIB_PCA with respect to n_{PCA} and the noise levels of AWGN. It can be found that the average CRR gradually improves as n_{PCA} increases. But when n_{PCA} reaches a certain value, the CRR remained unchanged. It can also be seen that the average CRR is constantly reduced when the level of Gaussian noise is increased.

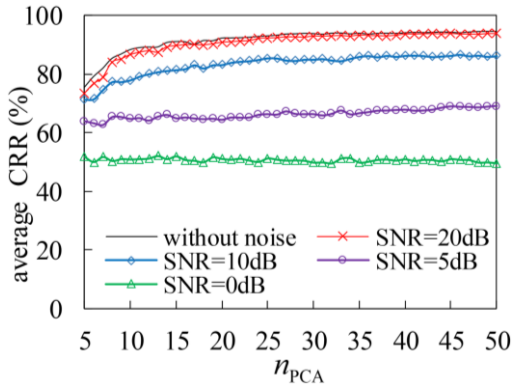

Fig. 12. The average CRR of three aircraft models with respect to n_{PCA} and the levels of AWGN.

To give insight into the confusion of the three aircraft in recognition process, Table 3 shows CRR when each aircraft is chosen as the testing target respectively. Here n_{PCA}=50. It can be noticed that the CRR is inversely proportional to the level of Gauss's noise, and it can be improved to a certain extent by projecting the MSIB features onto the lower-dimensional PCA space for recognition. It also can be found that the CRR of VFY-218 is higher than the other two. This is because the HRRPs of VFY-218 are obviously different, as shown in Fig. 5.

Table 3: Correct recognition rate of three aircraft models

		F15	F117	VFY-218
Without noise	MSIB	92.92	94.21	96.25
	MSIB_PCA	94.38	94.17	99.17
SNR= 20dB	MSIB	92.62	93.58	96.25
	MSIB_PCA	92.71	92.5	98.75
SNR= 10dB	MSIB	81.46	87.71	94.17
	MSIB_PCA	81.88	82.08	98.33
SNR= 5dB	MSIB	55.00	57.08	88.33
	MSIB_PCA	60.42	56.88	93.96
SNR= 0dB	MSIB	46.04	39.79	62.29
	MSIB_PCA	46.46	39.58	72.71

IV. CONCLUSION

In this paper, efficient wideband MRCS simulation has been presented for radar HRRP target recognition based on MSIB and PCA. Firstly, an efficient numerical approach has been proposed for the wideband MRCS from a target. The well-conditioned integral equation combined with the novel higher-order hierarchical divergence-conforming vector basis functions and the MLFMA has been utilized for efficient scattering analysis. The well-conditioned matrix equation can obtain rapid converging iterative solutions without preconditioning. Comparing with low-order techniques, the use of novel higher order hierarchical divergence-conforming vector basis function can greatly reduce the number of unknowns for a given problem. By using the low-rank property of the multiple RHS problem, the ACA based matrix compression method has been employed for efficient computation of MRCS. Compared with solving linear equations repeatedly at each angle with direct solution, the ACA based matrix compression method can greatly reduce the computation time. The GTD-based scattering model has been utilized for fast analysis of MRCS over a wide frequency band. By modeling a complex target as a summation of ideal scattering centers, large amount of calculation can be reduced. Finally, the one-dimensional MSIB features of HRRP have been extracted to constitute eigenvectors

for radar target recognition. To enhance the separation ability of radar target recognition, the MSIB features have been projected onto a lower-dimensional PCA space for recognition. Numerical examples prove that the proposed algorithm is feasible and efficient.

ACKNOWLEDGMENT

The work is supported by the National Natural Foundation of China (Grant No. 61401219). We would like to thank the sponsors.

REFERENCES

[1] S. P. Jacobs, *Automatic Target Recognition Using High-Resolution Radar Range Rrofiles*. Washington University, Washington, 1997.

[2] L. Du, H. He, and L. Zhao, "Noise robust radar HRRP target recognition based on scatterer matching algorithm," *IEEE Sensors Journal*, vol. 16, no. 6, pp. 1743-1753, Mar. 2016.

[3] H. W. Liu, B. Feng, and B. Chen, "Radar high-resolution range profiles target recognition based on stable dictionary learning," *IET Radar Sonar and Navigation*, vol. 10, no. 2, pp. 228-237, Feb. 2016.

[4] J. M. Song, C. C. Lu, and W. C. Chew, "Multilevel fast multipole algorithm for electromagnetic scattering by large complex objects," *IEEE Trans. Antennas Propagat.*, vol. 45, no. 10, pp. 1488-1493, 1997.

[5] X. C. Wei, Y. J. Zhang, and E. P. Li, "The hybridization of fast multipole method with asymptotic waveform evaluation for the fast mono-static RCS computation," *IEEE Trans. Antennas Propag.*, vol. 52, no. 2, pp. 605-607, Feb. 2004.

[6] R. D. Slone, J. F. Lee, and R. Lee, "Automating multipoint Galerkin AWE for a FEM fast frequency sweep," *IEEE Trans. Magn.*, vol. 38, no. 2, pp. 637-640, 2002.

[7] Z. W. Liu, R. S. Chen, and J. Q. Chen, "Adaptive sampling cubic-spline interpolation method for efficient calculation of monostatic RCS," *Microw. Opt. Technol. Lett.*, vol. 50, no. 3, pp. 751-755, 2008.

[8] J. Shaeffer, "Direct solve of electrically large integral equations for problem sizes to 1 M unknowns," *IEEE Trans. Antennas Propag.*, vol. 56, no. 8, pp. 2306-2313, 2008.

[9] Z. H. Fan, Z. W. Liu, D. Z. Ding, and R. S. Chen, "Preconditioning matrix interpolation technique for fast analysis of scattering over broad frequency Band," *IEEE Trans. Antennas Propag.*, vol. 58, no. 7, pp. 2484-2487, 2010.

[10] C. J. Reddy, M. D. Deshpande, C. R. Cockrell, and F. B. Beck, "Fast RCS computation over a frequency band using method of moments in conjunction with asymptotic waveform evaluation technique," *IEEE Trans. Antennas Propag.*, vol. 46, no. 8, pp. 1229-1233, Aug. 1998.

[11] G. Hislop, N. A. Ozdemir, C. Craeye, and D. G. Ovejero, "MoM matrix generation based on frequency and material independent reactions (FMIR-MoM)," *IEEE Trans. Antennas Propag.*, vol. 60, no. 12, pp.5777-5786, Dec. 2012.

[12] V. Chandran and S. L. Elgar, "Pattern recognition using invariants defined from higher order spectra-one-dimensional inputs," *IEEE Trans. Signal Proces.*, vol. 41, no. 1, pp. 205-212, Jan. 1993.

[13] J. K. Tugnait, "Detection of non-Gaussian signals using integrated polyspectrum," *IEEE Trans. Signal Proces.*, vol. 42, no. 11, pp. 3137-3149, Nov. 1994.

[14] X. J. Liao and Z. Bao, "Circularly integrated bispectra: Novel shift invariant features for high-resolution radar target recognition," *Electronics Letters*, vol. 34, no. 19, pp. 1879-1880, Sept. 1998.

[15] V. Chandran and S. L. Elgar, "Pattern recognition using invariants defined from higher order spectra-one-dimensional inputs," *IEEE Trans. Signal Proces.*, vol. 41, no. 1, pp. 205-212, Jan. 1993.

[16] V. Chandran and S. L. Elgar, "Pattern recognition using invariants defined from higher order spectra-one-dimensional inputs," *IEEE Trans. Signal Proces.*, vol. 41, no. 1, pp. 205-212, Jan. 1993.

[17] Y. Q. Hu, J. J. Ding, D. Z. Ding, and R. S. Chen, "Analysis of electromagnetic scattering from dielectric objects above a lossy half space by multiresolution preconditioned MLFMA," *IET Microwaves, Antennas & Propagation*, vol. 4, no. 2, pp. 232-239, Feb. 2010.

[18] P. Ylä-Oijala, M. Taskinen, and S. Järvenpää, "Analysis of surface integral equations in electro-magnetic scattering and radiation problems," *Engineering Analysis with Boundary Elements*, vol. 32, pp. 196-209, 2008.

[19] Y. Q. Hu, D. Z. Ding, Z. H. Fan, and R. S. Chen, "Well-conditioned MLFMA for electromagnetic scattering from dielectric objects above a lossy half-space," *Microwave and Optical Technology Letters*, vol. 52, no. 2, pp. 381-386, 2010.

[20] R. S. Chen, Y. Q. Hu, Z. H. Fan, D. Z. Ding, D. X. Wang, and E. K. N. Yung, "An efficient surface integral equation solution to EM scattering by chiral objects above a lossy half space," *IEEE Trans. Antennas Propagat.*, vol. 57, no. 11, pp. 3586-3593, 2009.

[21] P. Ylä-Oijala and M. Taskinen, "Application of combined field integral equation for electro-magnetic scattering by dielectric and composite objects," *IEEE Trans. Antennas Propagat.*, vol. 53, no. 3, pp. 1168-1173, Mar. 2005.

[22] R. D. Graglia, A. F. Peterson, F. P. Andriulli, "Curl-conforming hierarchical vector bases for triangles and tetrahedra," *IEEE Trans. Antennas*

Propagat., vol. 59, no. 3, pp. 950-959, 2011.

[23] L. P. Zha, Y. Q. Hu, and T. Su, "Efficient surface integral equation using hierarchical vector bases for complex EM scattering problems," *IEEE Trans. Antennas Propagat.*, vol. 60, no. 2, pp. 952-957, Feb. 2012.

[24] Z. P. Nie, W. Ma, Y. Ren, Y, Zhao, J. Hu, and Z. Zhao, "A wideband electromagnetic scattering analysis using MLFMA with higher order hierarchical vector basis functions," *IEEE Trans. Antennas Propag.*, vol. 57, no. 10, pp. 3169-3178, Oct. 2009.

[25] L. C. Potter, D. M. Chiang, R. Carriere, and M. J. Gerry, "A GTD-based parametric model for radar scattering," *IEEE Trans. Antennas Propagat.*, vol. 43, no. 10, pp. 1058-1067, Oct. 1995.

[26] L. C. Trintinalia, R. Bhalla, and H. Ling, "Scattering center parameterization of wide-angle backscattered data using adaptive Gaussian representation," *IEEE Trans. Antennas Propagat.*, vol. 45, no. 11, pp. 1664-1668, 1997.

[27] T. K. Sarkar and Odilon Pereira, "Using the matrix pencil method to estimate the parameters of a sum of complex exponentials," *IEEE Antennas and Propagation Magazine*, vol. 37, no. 1, pp. 48-55, 1995.

[28] T. K. Moon and W. C. Stirling, *Mathematical Methods and Algorithms for Signal Processing*, Prentice Hall, 1999.

[29] J. H. Jung and H. T. Kim, "Comparisons of four feature extraction approaches based on Fisher's linear discriminant criterion in radar target recognition," *Journal of Electromagnetic Waves and Applications, PIER*, vol. 21, no. 2, pp. 251-265, 2007.

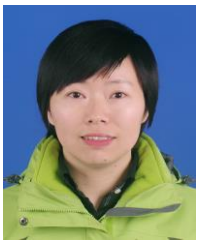

Yunqin Hu received Ph.D. degree in Information and Communication Engineering from Nanjing University of Science and Technology. During 2014, she was with the Electrical and Computer Engineering of Iowa State University as a visiting scholar. She is currently a Lecturer with the Communication Engineering of Nanjing University of Posts and Telecommunications. Her current research interests include computational electromagnetics, antennas and electromagnetic scattering and propagation in complex media.

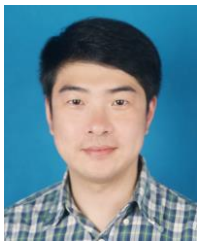

Ting Wan received the Ph.D. degree in Information and Communication Engineering from Nanjing University of Science and Technology.

He is currently an Associate Professor of Nanjing University of Posts and Telecommunications. His research interests include computational electromagnetics, electromagnetic scattering and radiation, and electromagnetic modeling of microwave/ millimeter wave integrated circuits.